

Prediction and model-assisted estimation of diameter distributions using
Norwegian national forest inventory and airborne laser scanning data

Janne Räty^{*1}, Rasmus Astrup¹ and Johannes Breidenbach^{*1}

¹Norwegian Institute of Bioeconomy Research (NIBIO), Division of Forest and Forest Resources,
National Forest Inventory, Høgskoleveien 8, 1433 Ås, Norway

ABSTRACT

Diameter at breast height (DBH) distributions offer valuable information for operational and strategic forest management decisions. We predicted DBH distributions using Norwegian national forest inventory and airborne laser scanning data in an 8.7 Mha study area and compared the predictive performance of parameter prediction methods using linear-mixed effects (PPM) and generalized linear-mixed models (GLM), and a k nearest neighbor (NN) approach. With PPM and GLM, it was assumed that the data follow a truncated Weibull distribution. While GLM resulted in slightly smaller errors than PPM, both were clearly outperformed by NN. We applied NN to study the variance of model-assisted (MA) estimates of the DBH distribution in the whole study area. The MA estimator yielded greater than or almost equal efficiencies as the direct estimator in 2 cm DBH classes (6, 8..., 50 cm) where relative efficiencies (REs) varied in the range of 0.97–1.63. RE was largest in the DBH classes ≤ 10 cm and decreased towards the right tail of the distribution. A forest mask and tree species map introduced further uncertainty beyond the DBH distribution model, which reduced REs to 0.97–1.50.

Keywords: airborne lidar, generalized linear models, linear mixed-effects models, most similar neighbor approach, Weibull distribution, number of stems

1 INTRODUCTION

Forest inventories provide essential information for the sustainable management of forest resources at different spatial levels. A key forest attribute is diameter at breast height (DBH) which is correlated with many other tree attributes, such as timber volume, biomass and timber assortments. Therefore, the distribution of DBHs (henceforth DBH distribution) is vital in the assessment of timber-related attributes in a forest. DBH distributions are also indicative of forest structural characteristics which may be relevant for biodiversity assessments (Valbuena et al. 2013). In operational forestry, the main purpose of DBH distributions is to characterize the trees of forest stands for the planning of forest management. The tree-level information is required, for example, in growth simulations when tree-level models are applied (Hynynen et al. 2002). The information associated with the tree dimensions is also important in the strategic planning of larger areas like municipalities, provinces or a country. These large-scale DBH distributions can be used to estimate, for example, biomass or timber assortment volumes. Time series of large-scale DBH distributions are useful in the monitoring of changes in forested areas (Coomes and Allen 2007, Henttonen et al. 2019).

There are several probability density functions that have been used in the characterization of DBH distributions. The most common functions are Beta (Loetsch et al. 1973), Johnson SB (Hafley and Schreuder 1977) and Weibull (Bailey and Dell 1973). The two-parameter Weibull distribution has achieved popularity because of its convenient mathematical properties and flexibility to characterize various distribution shapes, such as right- and left-skewed, and Gaussian-shaped distributions (Bailey and Dell 1973). For the same reasons, the focus of this study is on the Weibull distribution.

The parameters of the Weibull distribution can be obtained using the parameter prediction method (PPM) (Kilkki et al. 1989) or the parameter recovery method (PRM) (Burk and Newberry 1984, Siipilehto and Mehtätalo 2011). Both methods originate from traditional field-

based forest management inventories which today are vastly superseded by airborne laser scanning (ALS)-supported inventories following the area-based approach (ABA) (Næsset et al. 1997). The typical field dataset of ALS-supported inventories consists of sample plots with a full enumeration of DBHs (Næsset 2014, Maltamo and Packalen 2014).

PPM consists of three steps in ALS-supported forest inventories. First, Weibull distributions are fit to DBH distributions of individual sample plots (e.g. Bailey and Dell 1973). Second, each of the estimated parameters is regressed against predictor variables such as ALS metrics (Gobakken and Næsset 2004) or forest attributes which were themselves predicted using ALS metrics (Packalén and Maltamo 2008). Finally, the model is applied to a wall-to-wall data set of the predictor variables, typically consisting of grid cells with a similar size as the sample plots. An additional model for the stem frequency is needed to predict the stem frequency per DBH class given the predicted Weibull parameters.

PRM consists of two steps. First, recovery attributes such as basal area, mean DBH, stem frequency and moments/percentiles of the DBH distribution are predicted for grid cells using ALS metrics. Then, the mathematical relationships between the recovery attributes and parameters of the Weibull distribution are used to create a non-linear system of equations. This system is solved using a root-finding approach such as Newton-Raphson (Siipilehto and Mehtätalo 2013). Because a numerical solution is not always possible with PRM when using predicted recovery attributes (Mehtätalo et al. 2007), we focus on PPM below.

Breidenbach et al. (2008) adapted a variety of a generalized linear model (GLM, see Cao 2004) for the prediction of DBH distribution in an ALS-supported forest inventory. Due to the structure of the field data (concentric sample plots), they used several truncated Weibull distributions conditional to specific DBH ranges. The benefits of the approach are that the

estimation of the Weibull parameters can be carried out with a single-step in which the observed DBHs are regressed directly against ALS metrics.

One challenge of Weibull-based methods is that the basic formulations of probability density function cannot characterize multimodal DBH distributions (Zhang et al. 2001, Thomas et al. 2008). This is one of the reasons why the non-parametric nearest neighbor approach (NN) has been proposed for the prediction of DBH distributions in boreal ALS-based forest inventories, for example in Finland (Packalén and Maltamo 2008), Norway (Maltamo et al. 2009), and the United States (Mauro et al. 2019). NN enables the prediction of DBH distributions without any assumptions related to the shape of the distribution. Therefore, NN can predict multimodal and irregular DBH distributions. NN also enables the simultaneous prediction of DBH distributions and other forest attributes which yields consistent multivariate results (Packalén and Maltamo 2008). A disadvantage of NN is that it cannot extrapolate which may be problematic, if the field sample is not comprehensive enough (e.g. Breidenbach et al. 2012).

Only few studies examined the estimation of DBH distributions at larger scales like municipalities, regions, or countries (Magnussen and Renaud 2016, Henttonen et al. 2019). The precision of direct (field data-based) estimates of forest attributes can be improved by means of remotely sensed data (e.g. McRoberts and Tomppo 2007, Haakana et al. 2020). In the context of DBH distributions this has been investigated by Magnussen and Renaud (2016) who demonstrated that a combination of forest inventory and ALS data can be used to obtain model-assisted (MA) estimates of DBH distributions. They utilized multi-dimensional scaling (MDS) to link ALS data to the observed DBH distribution in four different study sites where the sample plot data were collected using stratified simple random sampling. The MDS approach is not scale dependent and it was applied both at the level of forest stands and at the level of strata. From the point of view of boreal forests, the limitation of the approach by Magnussen and

Renaud (2016) may be challenges with the prediction of stem frequency of small trees. They therefore did not consider suppressed trees and applied a DBH threshold of 17.5 cm.

We used Norwegian National Forest Inventory (NFI) and ALS data in the characterization of DBH distributions in an 8.7 Mha study area. Our objectives are i) to model DBH distributions at the plot level using ALS metrics and ii) to analyze whether using the model can result in efficiency gains in the estimates of the DBH distribution of the study area. For objective i), we compared PPM, GLM, and NN. The parametric approaches (PPM and GLM) utilized truncated Weibull distributions. As opposed to previous studies, we consider the hierarchical structure of the data using mixed-effects models in the parametric approaches.

2 MATERIALS

2.1 Study area

The 8.7 Mha study area is approximately located between 58° N and 66° N in Norway where ALS data were available from a national laser scanning campaign (Figure 1). The study area contains significant climatic gradients caused by the large latitudinal extend. Significant elevational variations are also typical in the mountainous topography of Norway. The most economic value of forest is associated with the coniferous tree species: Norway spruce (*Picea abies* [L.] Karst.) and Scots pine (*Pinus sylvestris* [L.]). There are also several deciduous species growing in the area. Among the deciduous species, the most dominant are birch species (*Betula spp* [L.]) (Breidenbach et al. 2020b).

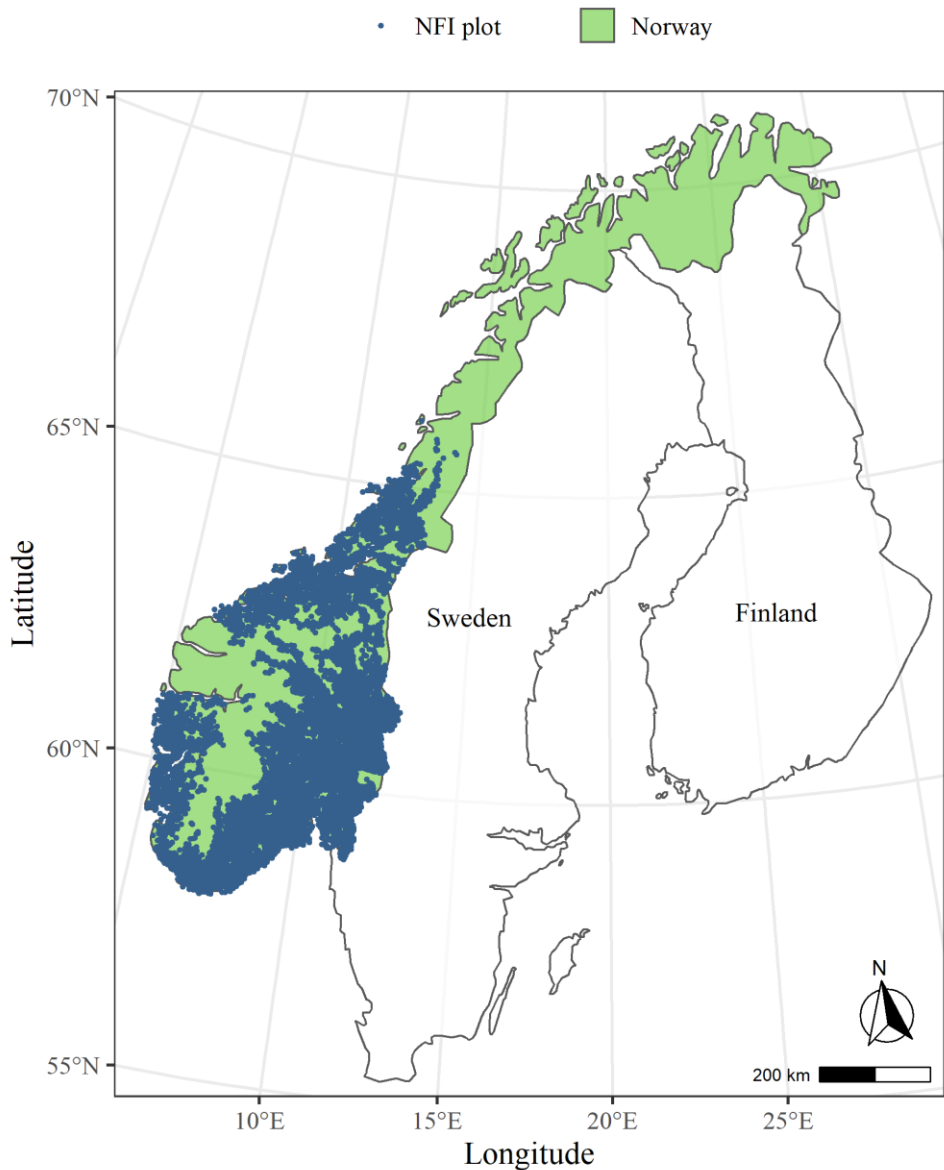


Figure 1. Approximate locations of the national forest inventory (NFI) field plots (n = 9615) used in this study.

2.2 Field data

Our field dataset consisted of NFI plots measured between 2014 and 2018 from the lowland design stratum of the study area (Breidenbach et al. 2020a). The locations of NFI field plots follows a systematic grid with a resolution of 3×3 km in the considered lowland design stratum resulting in a total of 9,615 sample plots within the study area. Altogether, 8,384 of the sample

plots were located within forest according to the NFI definition (10% crown cover and ability to reach 5 meters height). The NFI plots are circular plots with an area of 250 m². In plots with forest cover, DBH and species were recorded for each tree with a DBH \geq 5cm. For more detailed information related to the Norwegian NFI dataset, we refer to Breidenbach et al. (2020a).

Two datasets were created. The *modeling dataset* was used to compare the PPM, GLM, NN approaches. The efficiency gains of estimates supported by using the best modelling approach was analyzed using the *estimation dataset*.

The modeling dataset, for the comparison of the three approaches (PPM, GLM, NN), consisted of plots that were located in single-layered stands because PPM and GLM rely on a unimodal probability density function. We split the NFI data into three groups by dominant tree species (spruce, pine, and deciduous). The dominance of tree species was determined based on species-specific timber volumes, which means that usually trees from more than one species were present at the plots. Furthermore, we excluded plots with less than 5 measured trees or if they were located at the border of forest stands (split plots). The dataset consisted of 905, 813, and 259 plots in spruce, pine and deciduous forest, respectively. For these plots, observed DBH distributions were constructed using a 2 cm bin width. Statistics associated with the forest attributes of the modeling data are presented in Table 1.

The estimation dataset for the large-scale estimation of the DBH distribution as the stem frequency in 2 cm DBH classes consisted of all forested and non-forested plots in the study area (n = 9,615). A total of 60 evident outliers resulting from harvests between field and remotely-sensed data acquisitions were excluded and assumed missing at random. The outliers were inspected by visualizing ALS data and aerial images. A total of $n_F = 8,312$ sample plots were located within forest with 3,335, 3,338 and 2,015 plots in spruce, pine, and deciduous forest,

respectively. Characteristics of the estimation dataset (plots within forest) are shown in Table 1 and Figure 2.

Table 1. Characteristics of selected forest attributes in the modeling dataset and the estimation dataset. V – volume, G – basal area, N – stem frequency, DBH – diameter at breast height, DG – basal area weighted mean DBH, Hg – Lorey's height

Statistic	Dominant tree species	Modeling dataset				Estimation dataset			
		Mean	Sd	Min	Max	Mean	Sd	Min	Max
V ($\text{m}^3 \cdot \text{ha}^{-1}$)	Spruce	245.3	153.5	6.6	1000.4	146.2	141.1	0	1000.4
	Pine	163.6	93.0	11.4	615.1	103.1	95.6	0	702.2
	Deciduous	100.1	72.9	4.2	473.4	68.6	79.2	0	680.3
G ($\text{m}^2 \cdot \text{ha}^{-1}$)	Spruce	30.1	13.3	1.6	96.2	19.6	14.4	0	96.2
	Pine	22.5	9.8	2.6	59.6	15.2	11.3	0	79.1
	Deciduous	17.7	9.7	1.1	60.6	12.0	11.0	0	69.7
N (ha^{-1})	Spruce	1262	647	200	4560	1030	698	0	5000
	Pine	785	481	200	4200	662	522	0	4520
	Deciduous	1336	863	200	5560	1012	839	0	5560
DG (cm)	Spruce	23.0	6.2	8.5	47.0	20.3	7.5	5.0	60.6
	Pine	25.2	6.0	10.7	49.3	23.7	7.6	5.2	70.0
	Deciduous	17.5	6.4	7.1	51.3	15.6	7.2	5.0	155.0
Hg (m)	Spruce	16.0	4.0	5.6	28.8	13.4	4.8	3.2	32.3
	Pine	14.5	3.3	6.6	27.0	12.3	4.2	2.3	70.1
	Deciduous	10.9	3.5	4.9	26.0	9.8	4.1	2.7	26.6
Tree-level DBH (cm)	Spruce	15.4	8.2	5.0	79.8	13.4	7.9	5.0	79.8
	Pine	16.9	9.0	5.0	68.0	14.6	8.9	5.0	96.0
	Deciduous	11.5	6.0	5.0	58.0	10.7	6.0	5.0	155.0

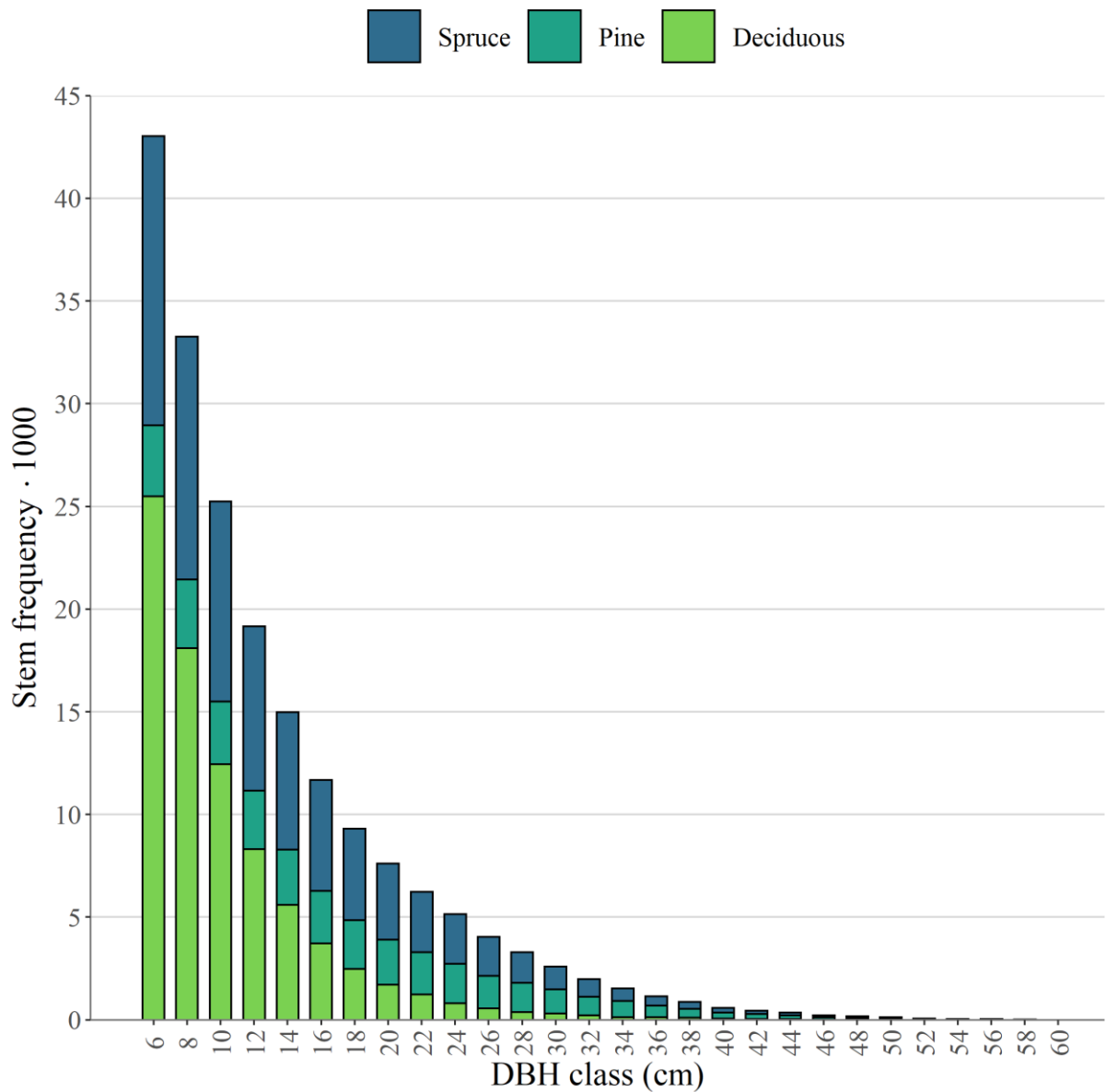


Figure 2. DBH distribution of all trees in the forested plots (estimation dataset).

2.3 Airborne laser scanning data and extracted metrics

The acquisition of ALS data was carried out between 2010 and 2018. The study area was covered by several ALS campaigns, which means that the flight parameters differ across the study area. The mean pulse density varied between 2–5 points per square meter. A digital terrain model (DTM, 1×1 m) was created using the last returns of ALS datasets (Kartverket 2019).

The orthometric height measurements of the ALS point cloud were normalized to above ground heights by subtracting the DTM elevation from the ALS elevation measurements.

The explanatory variables extracted from the ALS data for field plots comprised height, intensity, and echo proportion metrics. The height metrics consist of minimum, maximum, mean, variance and coefficient of variation, skewness and kurtosis, as well as height percentiles and densities. For density metrics, the height range from the ground to the 95% percentile was divided into 10 height slices of equal size (starting from slice 0 which is the closest to the ground level). The densities were computed as the proportion of returns above the height slices 0, 2, 4, 6, 8, and 9 to all returns (without echo categorization). In addition, the proportion of echoes above 2 meters was computed. The intensity metrics were computed based on the intensity recordings of ALS data and consisted of variance, coefficient of variation, and ratio between the mean of ground echo intensities and the mean of vegetation echo intensities. The metrics were computed by echo categories: first, last, and all. We extracted altogether 23 statistical metrics from the ALS data per echo category. Table 2 shows the extracted metrics and their abbreviations.

Table 2. Metrics extracted from the ALS data. The metrics were computed by echo categories first, last, and all.

Abbreviation	Description
<i>Height metrics</i>	
hmin, hmax, hmean, hvar, hcv	Minimum, maximum, mean, variance, coefficient of variation
hskew, hkurt	Skewness and kurtosis
h10, h25, h50, h75, h90, h95	Height percentiles for 10%, 25%,..., 95%
d0, d2, d4, d6, d8, d9	Height densities
<i>Intensity metrics</i>	
ivar, icv, igratio	Variance, coefficient of variation, ratio between the mean of ground echo intensities and the mean of vegetation echo intensities
<i>Proportion metrics</i>	
proph	Proportion of echoes above 2 meters

3 METHODS

3.1 Prediction of DBH distributions

3.1.1 Parameter prediction method using linear mixed-effects models (PPM)

We applied a left-truncated two-parameter Weibull function (Zutter et al. 1986) in the modeling of DBH distributions because the dataset did not include trees with a DBH < 5 cm. The truncated two-parameter Weibull probability distribution where x is a DBH is

$$f(x| c, b) = \begin{cases} \frac{c}{b} \left(\frac{x}{b}\right)^{c-1} e^{\left[\left(\frac{T}{b}\right)^c - \left(\frac{x}{b}\right)^c\right]}, & x \geq T \\ 0, & x < T \end{cases} \quad (1)$$

where T is a fixed left-truncation point (5 cm), c is a shape parameter, b ($T < b$) is a scale parameter.

The estimates of Weibull parameters are needed for each sample plot in order to construct regression models for the parameters. We estimated the parameters of Weibull distribution by maximizing the log-likelihood function. The log-likelihood function for plot j is maximized given the Weibull parameters (c and b)

$$\log(L_j) = \sum_{k=1}^{n_j} \log(f(x_k|c, b)) \quad (2)$$

where n_j is the stem frequency in plot j and $f(\cdot)$ is a truncated Weibull probability distribution (Eq. 1) and x_k refers to the observed DBHs in a plot. This approach is referred to as the maximum likelihood (ML) method (Bailey and Dell 1973, Mehtätalo and Lappi 2020 p. 337–338). We used the *mle* function of the package *stats4* (R Core Team 2020) in *R* (R Core Team 2020) for the ML estimation of the plot-level Weibull parameters.

Because the field data have a hierarchical structure (NFI plots within ALS project), we fitted linear mixed-effects models with random intercepts for the shape and scale parameter of the Weibull distribution. The coefficients were estimated using the restricted maximum likelihood approach (e.g. Fahrmeir et al. 2013 p. 109), and the models were restricted to the $p=3$ most important predictor variables

$$y_{lij} = b_{li} + \beta_0 + \beta_1 x_{ij}^{(1)} + \cdots + \beta_p x_{ij}^{(p)} + \epsilon_{ij} \quad (3)$$

where y_{lij} is the response variable $l=\{\text{shape (c), scale (b)}\}$ predicted at plot j using Eq. (2) in ALS project i , $\beta_0 + \beta_1 x_{ij}^{(1)} + \cdots + \beta_p x_{ij}^{(p)}$ is the fixed part of the model in which the β s are the coefficients to be estimated and $x_{ij}^{(p)}$ are predictor variables, $b_{li} + \epsilon_{ij}$ is the random part of the model in which $b_{li} \sim N(0, \sigma_b^2)$ represents the random part of the intercept in ALS project i and

$\epsilon_{ij} \sim N(0, \sigma^2)$ represents the residual error of plot j in project i. We used the *nlme* package (Pinheiro et al. 2020) for the estimation of the model parameters. Ultimately, we transformed the predicted Weibull distributions to DBH distributions (i.e. histograms) with a bin width of 2 cm. Because of the small number of trees with a DBH > 50 cm (Figure 2), we show results for DBH classes with mid-points of 6-50 cm. The transformation was based on the cumulative Weibull distribution function and observed stem frequencies.

3.1.2 Parameter prediction using generalized linear models (GLM)

A GLM-like framework (Cao 2004; Mehtätalo and Lappi 2020, p. 370–373), simply denoted as GLM in the following, was used to construct parameter models that directly linked the measured DBHs and ALS metrics (Breidenbach et al. 2008). We applied the truncated Weibull distribution described in Eq. 1 and maximized the likelihood function

$$\log(L) = \sum_{j=1}^n \log(L_j) \quad (4)$$

for the Weibull parameters $\theta_{lijk} = \{b, c\}$ by optimizing the parameters of the regression function

$$\theta_{lijk} = b_{li} + b_{lij} + \beta_0 + \beta_1 x_{ijk}^{(1)} + \cdots + \beta_p x_{ijk}^{(p)} \quad (5)$$

where n is the number of plots, b_{li} is a random effect at the ALS-project level and b_{lij} is a plot-level random effect. It may be noted that all predictor variables for trees at a plot are identical.

The model for shape and scale parameters were fitted simultaneously by maximizing the penalized likelihood implemented in the *gamlss* package (Rigby and Stasinopoulos 2005) in the R environment (R Core Team 2020). We ignored the grouping of plots within ALS projects after preliminary analysis because of numeric instability. That means, as opposed to PPM, an ALS project-level random effect (b_{li}) was not included. A random intercept was, however, added at the plot-level (b_{lij}) to consider the dependence of trees and predictor variables within

a sample plot. Ultimately, we transformed the predicted Weibull distributions to DBH distributions (i.e. histograms) as described for PPM.

3.1.3 Nearest neighbor approach

NN is not based on any theoretical distributional forms and the resulting distribution is constructed directly from the reference data. For NN, the user has to choose the number of nearest neighbors (k), the number of predictor variables (p), the response configuration, and a distance metric. After preliminary analysis, we set k=p=5. The response configuration consisted of basal area, stem frequency, basal area weighted mean DBH and Lorey's height.

We used the most similar neighbor (MSN) distance, which is based on the canonical correlation analysis between the response and predictor variables (Moeur and Stage 1995). The squared MSN distance between reference u and target j observation derived from canonical correlation analysis is as follows:

$$d_{uj}^2 = \frac{(x_u - x_j) \Gamma \Lambda^2 \Gamma' (x_u - x_j)'}{1 \times p \quad p \times p \quad p \times 1} \quad (6)$$

Where d_{uj}^2 is the squared MSN distance, x_u and x_j are row vectors of predictor variables for training and target plots, Γ is a matrix of canonical coefficients of predictor variables, and Λ^2 is a diagonal matrix of squared canonical correlations.

We inverted the distances d_{uj}^2 to weight the reference tree lists for the target observations. The tree lists were transformed to DBH distributions with a bin width of 2 cm. These DBH distributions include the predicted stem frequency which was not the case with PPM and GLM. In order to compare the performance of NN with PPM and GLM, we converted the NN-based DBH distributions to match with the observed stem frequency. In the MA estimation, the stem frequencies were predicted using the NN model. NN was implemented using the *yaImpute* package (Crookston and Finley 2007) in R (R Core Team 2020). The NN-based DBH

distribution usually results in spikes and pits (Strunk et al. 2017). Therefore, we smoothed the NN-based DBH distributions with a 3-bin moving average.

3.1.4 Selection of predictor variables

We used the same predictor variables in PPM and GLM, which enabled to trace their performance differences. The predictor variables were selected in PPM which comprised two steps: an automatized step using an optimization algorithm and manual step for the final evaluation of the model fits. The automatized step was based on the heuristic optimization algorithm, known as simulated annealing (Kirkpatrick et al. 1983, Packalén et al. 2012), which minimizes a cost function by repeatedly fitting the model and randomly changing the combination of predictor variables. The initial temperature, the number of iterations per temperature, and a cooling factor determined the number of iterations. The cooling factor (value < 1) is used to cool the system by multiplying the current temperature value. The temperature value determines the probability to accept a worse solution. The cost function was the root-mean-squared error (RMSE, see section 3.4) associated with the response variable.

In case of PPM and GLM, the automatized step was used to reduce the number of predictor variable candidates. The manual step included the visual and numerical assessments related to the model fit statistics. Based on initial analysis, three predictor variables were selected for each Weibull parameter.

In case of NN, we only applied the automatized step. We repeated the selection of predictor variables five times in order to observe the fluctuation in the ultimate cost value caused by the heuristic optimization. We selected the repetition that resulted in the smallest cost value. The number of predictor variables was five.

3.2 Estimation of the study-area DBH distribution

3.2.1 Direct estimation of DBH distributions

We follow the notation of Breidenbach et al. (2020b) who described the estimators for estimating forest area by tree species over all Norwegian NFI design strata. The direct estimator for the total stem frequency within a given DBH class is

$$\hat{t} = \sum_{i=1}^n \frac{y_i}{\pi_i} \quad (7)$$

where n is the number of sample plots, y_i is the observed stem frequency within a DBH class for sample plot i , and π_i is the inclusion probability i.e. the inverse of the sampling weight. In our case, π_i is equal for all sample plots.

The variance of the estimate is the sample variance divided by the number of sample plots

$$\widehat{Var}(\hat{t}) = \frac{\sum_{i=1}^n (y_i - \bar{y})^2}{n(n-1)} \quad (8)$$

where \bar{y} is the mean of the observed stem frequency within a DBH class.

The standard error of the estimate is

$$SE(\hat{t}) = \sqrt{\widehat{Var}(\hat{t})} \quad (9)$$

3.2.2 Model-assisted estimation of DBH distributions

The MA estimator for stem frequency in a given DBH class is

$$\hat{t}_{MA} = \tilde{t} + \hat{t}_C \quad (10)$$

where \tilde{t} is the synthetic estimate of stem frequency, and \hat{t}_C is an estimated correction factor.

The estimate of the correction factor (\hat{t}_C) that is used to correct systematic errors in the predictions is

$$\hat{t}_C = \sum_{i=1}^n \frac{e_i}{\pi_i} \quad (11)$$

where $e_i = y_i - \hat{y}_i$ is a residual and \hat{y}_i is the predicted stem frequency within a DBH class. We carried out the predictions following the principle in which the target plot was never in the training data of the model (cf. leave-one-out cross validation).

An estimate of the variance of the MA estimate is

$$\widehat{Var}(\hat{t}_{MA}) = \frac{\sum_{i=1}^n (e_i - \bar{e})^2}{n(n-1)} \quad (12)$$

where \bar{e} is the mean of the residuals.

First, the MA estimator was applied using the known, field-observed forest definition and dominant tree species to describe the theoretical precision benefit of the MA estimation compared to direct estimation. Ultimately, we utilized an available forest mask and tree species map in order to demonstrate the efficiency associated with the practical estimation procedure. The forest mask had an overall accuracy (OA) of 92% while the tree species map had an OA 74% and 90% on plot and stand-level, respectively. For more information related to the tree species map and forest mask, we refer to Breidenbach et al. (2020b). An error in the forest mask has the effect that a forested plot is treated as a non-forest plot (absolute e_i equals to the observed stem frequency) or vice versa (absolute e_i equals to the predicted stem frequency). An error in the tree species map has the effect that a sub-optimal model (stratified NN models) is used for the prediction of the DBH distribution at a plot.

3.3 Evaluation of the models and estimators

We predicted DBH distributions using the leave-one-out cross validation and used a bin width of 2 cm in the performance assessments. We computed RMSE (Eq. 13) and mean difference (MD, Eq. 14) associated with each DBH class. Relative RMSEs (Eq. 13 divided by the observed mean) were also computed for the predicted Weibull parameters (scale and shape).

$$RMSE = \sqrt{\frac{\sum_{i=1}^n (y_i - \hat{y}_i)^2}{n}} \quad (13)$$

$$MD = \frac{\sum_{i=1}^n (y_i - \hat{y}_i)}{n} \quad (14)$$

In the estimation at the level of study area, we used the half width of 95 % confidence intervals and the relative efficiency (RE) in order to compare the efficiency of the direct and MA estimators

$$RE = \frac{\widehat{Var}(\hat{t})}{\widehat{Var}(\hat{t}_{MA})}. \quad (15)$$

In case of simple random sampling (SRS), the interpretation of RE is that the SRS with [sample size] = RE \times [original sample size] produces a similar variance as the model-assisted estimate. It should be noted that the Norwegian NFI is based on the systematic sampling design, and therefore the applied estimators overestimate variances due to their assumption of SRS design (Magnussen et al. 2020).

4 RESULTS

4.1 Prediction of DBH distributions

In this section, we only consider the results associated with the modeling of DBH distributions in the spruce-dominated plots (modeling dataset), which also comprises the majority of timber

volume in the study area. The findings were generally comparable between the dominant species groups, and, for the sake of clarity, the results associated with the pine- and deciduous-dominated plots are only shortly presented in Appendix.

The parameter estimates associated with PPM and GLM are presented in Table 3. The prediction of Weibull scale and shape parameters using PPM resulted in the relative RMSEs of 29.9% and 40.3%, respectively. With PPM, the random effect at the level of ALS project was beneficial for the scale parameter, but not for the shape parameter, in terms of Akaike information criterion (AIC). The random effect was nonetheless included in the both models for consistency. While $\text{proph}_{\text{first}}$ and $\text{hskew}_{\text{first}}$ were selected for both parameters, h95_{all} and $\text{hcv}_{\text{first}}$ were selected for scale and shape, respectively. However, the selected predictor variables allow for a reasonable physical interpretation as they describe the shape and scale of the ALS height distribution which is related to the DBH distribution. For NN, the following predictor variables were selected: $\text{hmean}_{\text{first}}$, h75_{all} , h95_{all} , $\text{proph}_{\text{first}}$, $\text{hskew}_{\text{last}}$.

Table 3. Parameter estimates and their standard errors/confidence intervals (SE/CI) associated with the linear mixed-effects models (PPM) and generalized linear models (GLM) for Weibull scale and shape parameters. Please refer to Table 2 for the abbreviations of predictor variables.

L – lower bound, U – upper bound

PPM				GLM				
scale		shape		scale		shape		
Est.	SE	Est.	SE	Est.	SE	Est.	SE	
Intercept	18.30	1.72	2.12	0.74	2.60	0.03	1.98	0.16
proph _{first}	-22.94	2.23	-2.13	0.66	-1.01	0.03	-1.82	0.13
hskew _{first}	-4.16	0.52	-1.65	0.11	-0.16	0.01	-0.56	0.02
h95 _{all}	0.95	0.05	-	-	0.06	<0.01	-	-
hcv _{first}	-	-	2.04	0.40	-	-	0.04	0.09
		95% CI			95% CI			
		Est. [L, U]			Est. [L, U]			
σ_b *	1.13	[0.73, 1.74]	0.08	[0.02, 0.42]	0.19	[0.18, 0.20]	0.20	[0.19, 0.22]
σ	4.82	[4.59, 5.06]	0.89	[0.85, 0.93]	-	-	-	-

* Note: ALS project-area random effect for PPM and plot-level random effect for GLM

NN provided smaller absolute errors than PPM and GLM when considering DBH distributions at the level of all spruce-dominated plots (Figure 3). The results showed that PPM and GLM performed similarly when looking at the distribution of absolute residuals in Figure 3. The sum of absolute residuals (DBH classes 6 – 50 cm) at the level of spruce-dominated plot group were 3,891; 3,489 and 929 stems for PPM, GLM and NN, respectively. Figure 3 and 4 describe the goodness of the predicted DBH distributions, and they show that systematic errors in the left

tail of the DBH distribution and between DBH classes 12–20 cm are apparent for the parametric approaches.

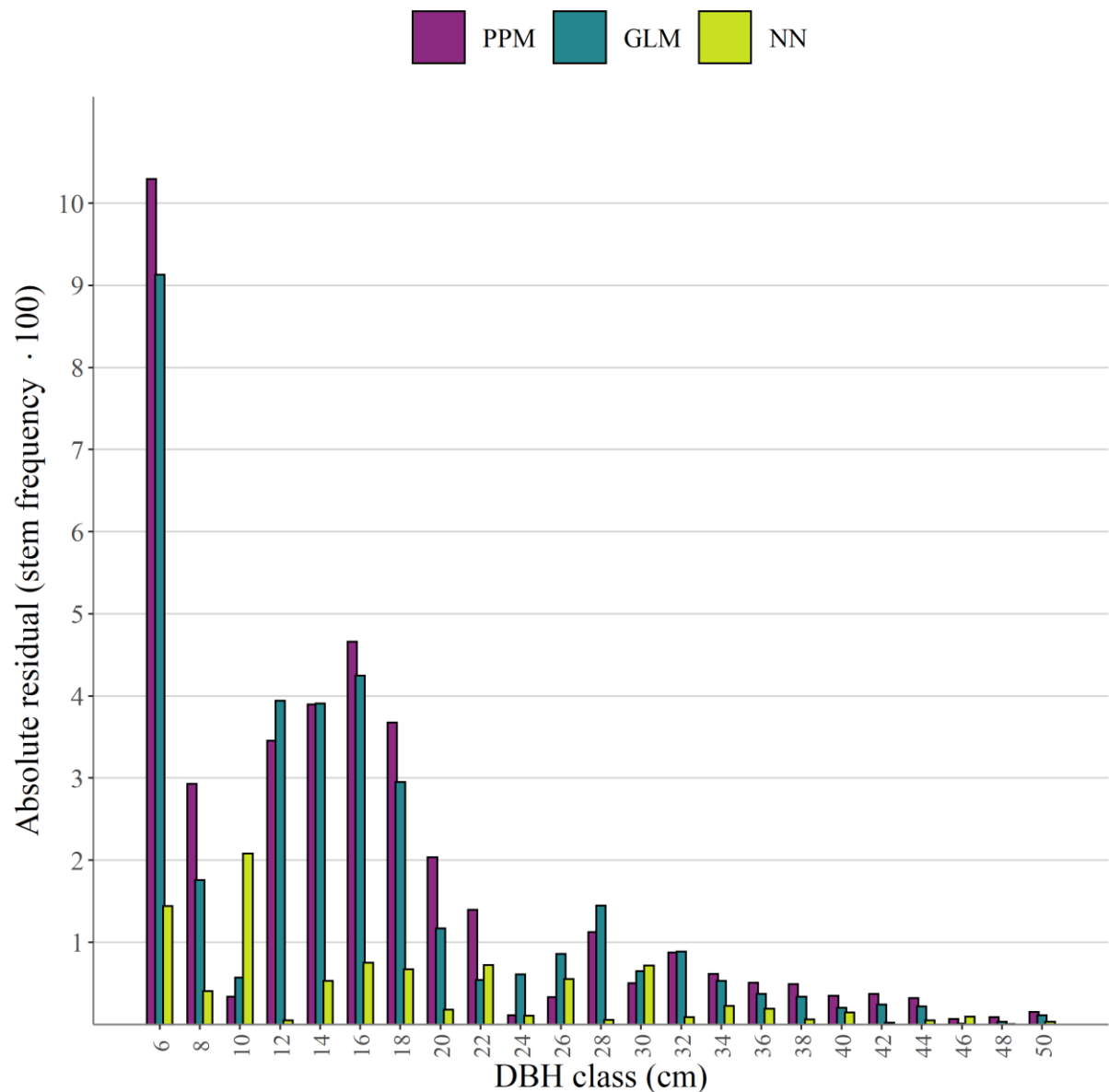


Figure 3. Absolute residuals of DBH distribution summed over all spruce-dominated plots (n = 905). PPM= parameter prediction method with linear mixed-effects models, GLM = generalized linear models and NN = nearest neighbor approach

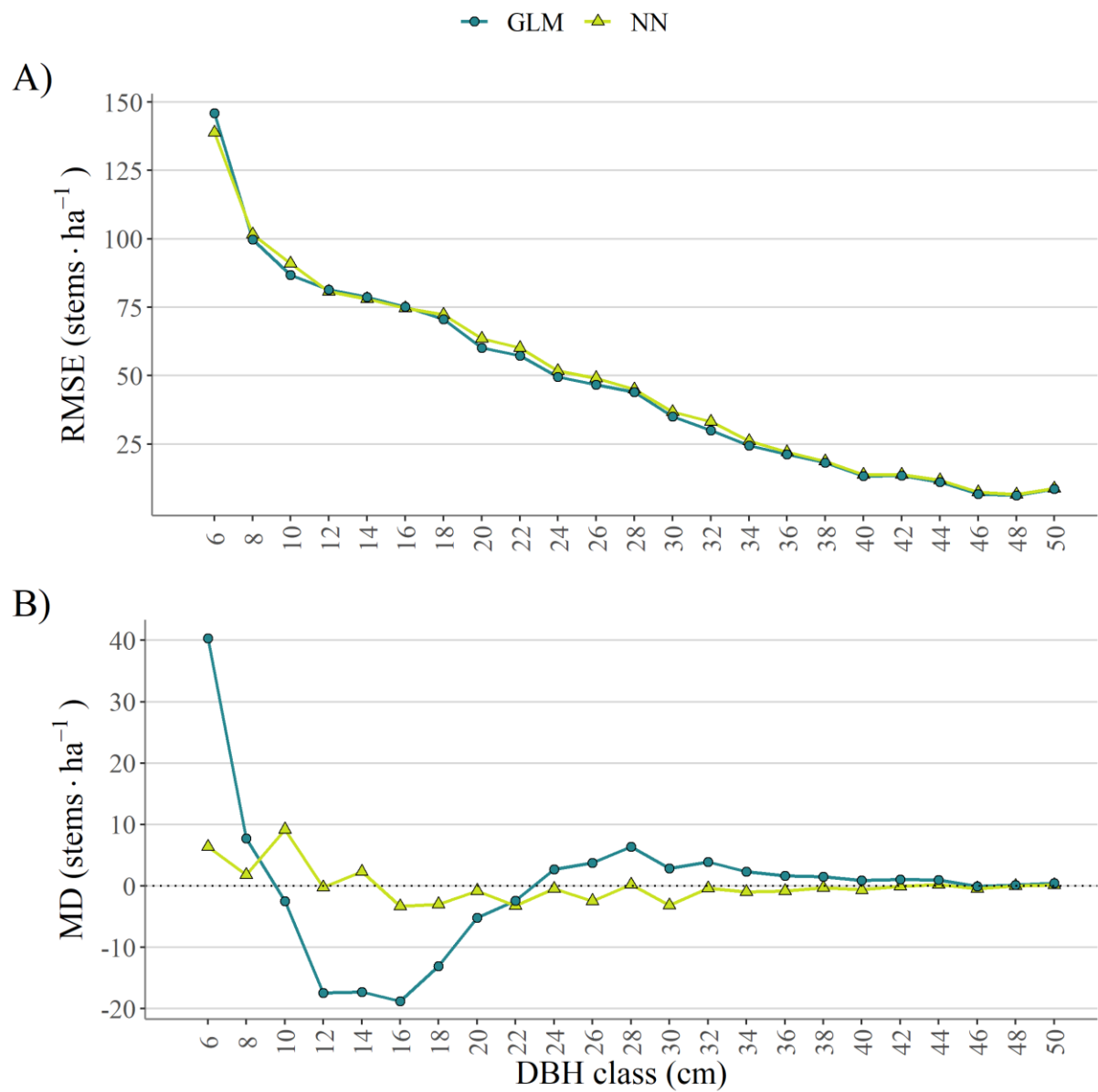


Figure 4. Root mean square error (RMSE) and mean difference (MD) associated with the predicted stem frequencies of the DBH classes in the spruce-dominated plots ($n = 905$). GLM – generalized linear model, NN – Nearest neighbor approach

4.2 Estimation of DBH distributions in the study area

The results presented in section 4.1 showed that NN outperformed GLM and PPM, and NN was therefore used for the MA estimation of DBH distribution for the study area. The comparison of GLM, PPM and NN was based on a simplified dataset that was optimized for the parametric approaches. The simplified dataset did not include multi-layered forests, plots with less than 5 trees or split plots. Because estimates are required for all forests including those that were challenging for the parametric approaches, new NN models for spruce, pine, and deciduous forest were trained using all ($n = 8,312$) forested plots (Table 1, estimation dataset). A total of 188 forested plots without measured trees (usually young forests with trees below the DBH threshold), were included in each dataset of spruce, pine, and deciduous forest since the dominant tree species was undefined. The predictor variables of these NN models are presented in Table 4. Figure 5A shows that the RMSE values were slightly larger than in the model comparison (Figure 4A) while the MD values presented in Figure 5B were in line with the results obtained during model comparison (Figure 4B).

Table 4. Predictor variables of the nearest neighbor approach (NN) by dominant tree species.

Dominant tree species	Predictor variables
Norway spruce	$hmean_{first}$, $h75_{all}$, $h95_{all}$, $proph_{first}$, $hskew_{last}$
Scots pine	$h25_{first}$, $h75_{all}$, $h95_{first}$, $d2_{all}$, $d6_{first}$,
Deciduous species	$h95_{all}$, $d0_{first}$, $d2_{all}$, $d4_{first}$, $hskew_{first}$

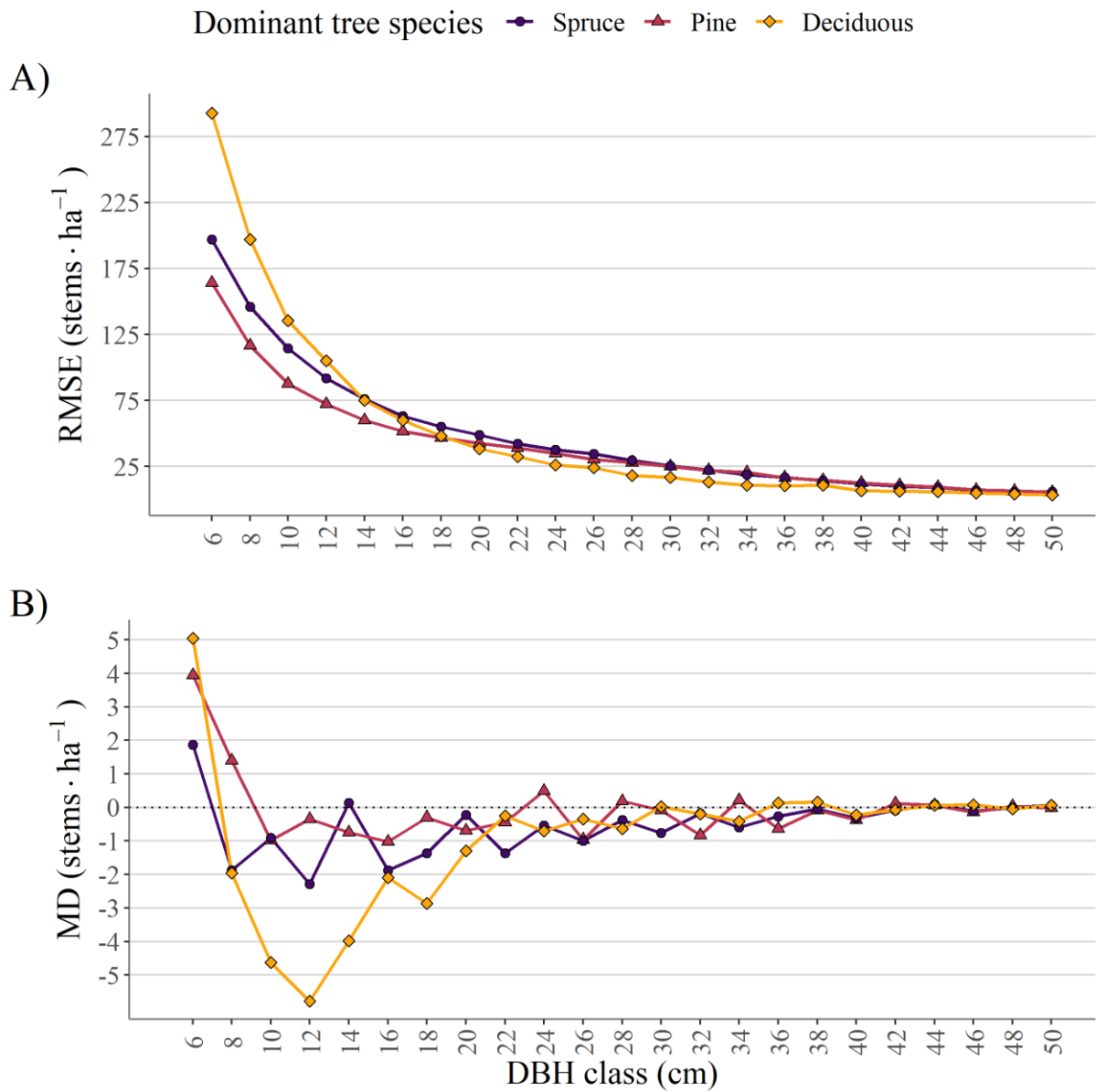


Figure 5. Evaluation of the nearest neighbor models used for the model-assisted estimation. A) shows root mean square error (RMSE) and B) mean difference (MD) associated with the predicted stem frequencies of the DBH classes in the plots dominated by spruce ($n = 3,335$), pine ($n = 3,338$), and deciduous ($n = 2,015$).

The efficiency assessments associated with the estimates of DBH classes are presented in Table 5 and Figure 6. The correction factors were larger in the left tail than in the right tail of the estimated DBH distribution. The correction factors associated with the small DBH classes were

larger with the forest mask and tree species map. MA estimation was more efficient than direct estimation in the DBH classes ≤ 46 cm. The RE values were slightly smaller than 1.00 in the DBH classes > 46 cm. Uncertainties in the forest mask and tree species map reduced the RE values which were nonetheless ≥ 0.97 for all DBH classes. The RE value associated with the MA estimate of total stem frequency was 2.56 (2.06 given forest mask and predicted tree species map).

Table 5. Characteristics associated with the direct and model-assisted estimation of the DBH distribution within the study area. Model-assisted estimates were computed with the observed tree species and observed forest/non-forest information, and with a tree species map and forest mask (in parenthesis). \hat{t} refers to the direct estimate of stem frequency, \hat{t}_{MA} refers to the model-assisted estimate.

DBH class (cm) *	Direct estimate \hat{t} (10^9 stems)	Half 95% CI(\hat{t}) (%)	Half 95% CI(\hat{t}_{MA}) (%)	Correction factor \hat{t}_C (10^6 stems)	DBH class (cm) *	Direct estimate \hat{t} (10^9 stems)	Half 95% CI(\hat{t}) (%)	Half 95% CI(\hat{t}_{MA}) (%)	Correction factor \hat{t}_C (10^6 stems)
6	1.56	2.71	2.23 (2.33)	48.96 (148.40)	30	0.09	4.59	4.13 (4.19)	-2.17 (0.54)
8	1.20	2.56	2.03 (2.13)	9.84 (79.86)	32	0.07	5.18	4.70 (4.72)	-3.25 (-0.83)
10	0.91	2.53	1.99 (2.07)	-5.31 (39.30)	34	0.06	5.70	5.34 (5.38)	-1.81 (0.38)
12	0.69	2.58	2.09 (2.17)	-12.98 (15.38)	36	0.04	6.37	6.09 (6.11)	-2.40 (-0.34)
14	0.54	2.63	2.13 (2.23)	-5.82 (11.32)	38	0.03	7.25	7.07 (7.10)	-0.07 (1.21)
16	0.42	2.77	2.27 (2.35)	-10.04 (1.41)	40	0.02	8.83	8.7 (8.74)	-2.43 (-1.57)
18	0.34	2.97	2.46 (2.53)	-8.50 (-1.72)	42	0.02	9.74	9.6 (9.64)	-0.01 (0.31)
20	0.28	3.16	2.64 (2.71)	-4.01 (0.26)	44	0.01	11.19	11.11 (11.08)	0.58 (0.88)
22	0.23	3.34	2.83 (2.90)	-4.95 (-1.01)	46	0.01	13.73	13.59 (13.61)	-0.56 (-0.33)
24	0.19	3.50	3.02 (3.08)	-0.71 (2.62)	48	0.01	15.21	15.38 (15.37)	-0.01 (0.26)
26	0.15	3.97	3.46 (3.53)	-6.04 (-2.28)	50	<0.01	18.99	19.18 (19.12)	0.26 (0.39)
28	0.12	4.21	3.71 (3.74)	-1.53 (1.26)	All	6.99	1.78	1.11 (1.23)	97.58 (395.69)

* DBH class refers to the middle of DBH class (bin width: 2cm)

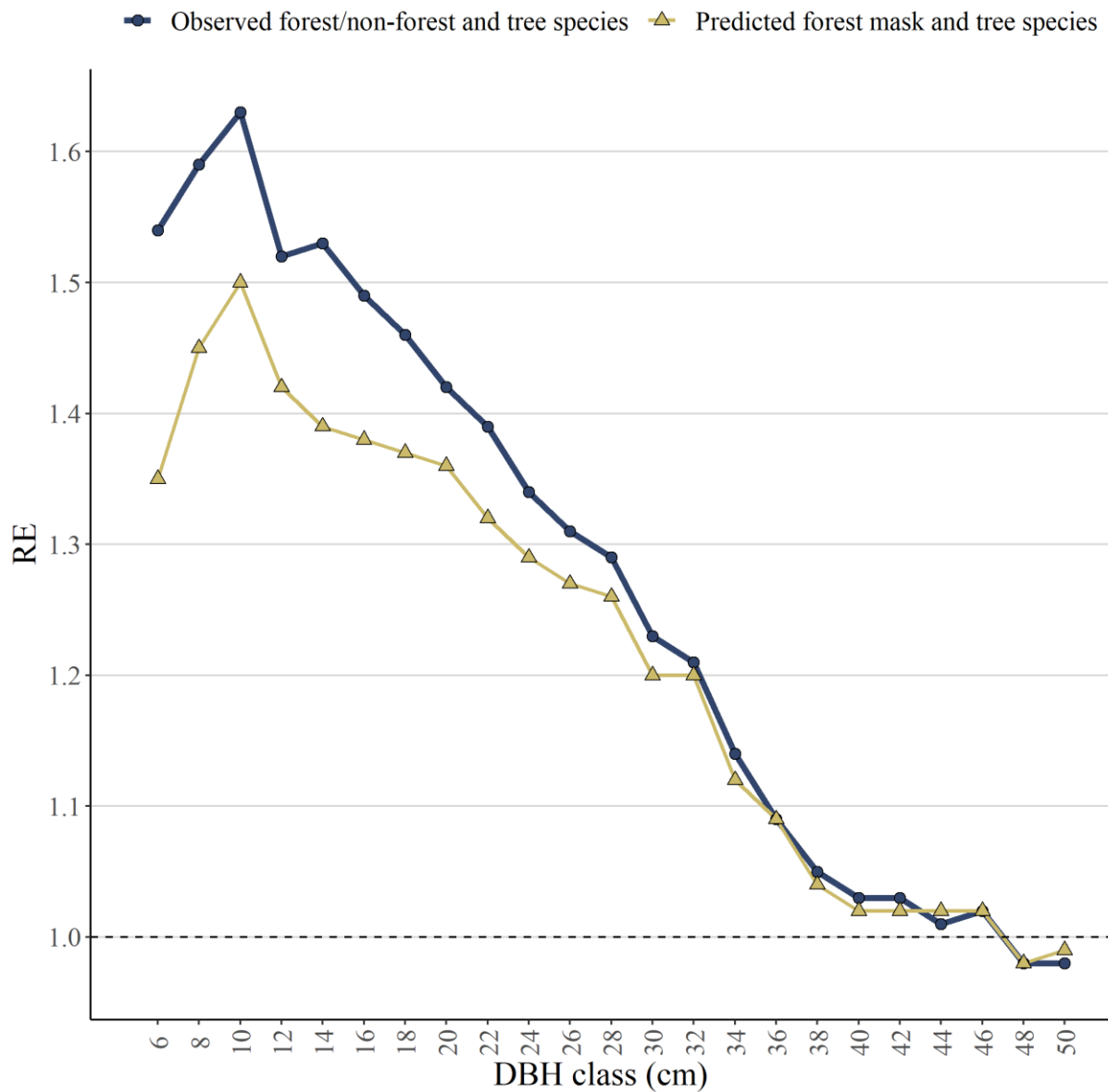


Figure 6. Relative efficiency (RE) of the model-assisted estimator.

5 DISCUSSION

Our findings indicated that the GLM performed slightly better than PPM in the prediction of DBH distributions. Nonetheless, the GLM approach has not achieved popularity in the prediction of DBH distributions in ALS-based forest inventories so far. Breidenbach et al. (2008) predicted DBH distributions using GLM and ALS data but they did not consider the clustered structure of the data. Because trees observed at one plot are not independent of each

other, the standard errors obtained by Breidenbach et al. (2008) were therefore too small which impeded variable selection. This issue was resolved here by adding a plot-level random effect.

The advantage of GLM is that it is a single-step approach, and therefore the estimation of Weibull parameters in the observed plot data is not needed like with PPM. In order to reasonably estimate the Weibull parameters at a plot, a sufficient number of DBH measurements is required. In some cases, the lack of trees may be an issue with relatively small plot sizes (e.g. 250 m²) often used in forest inventories. Furthermore, additive smoothing terms may improve the predictive performance of the GLM which would then be a generalized additive model (GAM) (Rigby and Stasinopoulos 2005). In preliminary analysis, smoothing terms did, however, not improve the predictive performance of the models in our case.

The dominating shape of DBH distributions in the study area was right-skewed. We also noticed that in some cases the shape of the observed DBH distributions was slightly bi-modal, which may partly explain the overpredictions observed with PPM and GLM in the DBH classes 12–20 cm. Bi-modal distribution functions may outperform unimodal distribution functions in forests where the DBH distribution has a bi-modal shape (Zhang et al. 2001, Thomas et al. 2008). However, the prediction of parameters for bi-modal distributions using ALS data is challenging even in case of clearly bi-modal DBH distributions (Thomas et al. 2008). Our findings indicated that it is difficult to find powerful predictor variables especially for the model of shape parameter. An alternative, as we showed, is to use NN which characterizes DBH distributions without an assumption regarding the form of distribution.

Our findings are generally in line with Packalén and Maltamo (2008) who reported that NN outperformed PPM in managed boreal forests. However, they focused on the prediction of species-specific DBH distributions and predicted Weibull parameters based on ALS-predicted forest attributes. The application of non-parametric approaches, such as NN, is justified by the

greater flexibility of characterizing different distribution shapes than unimodal probability functions. In the selection of the modeling approach, it is worth noting that the shapes of DBH distributions are affected, for example, by silvicultural activity (Rouvinen and Kuuluvainen 2005). For example, Maltamo et al. (2018) studied homogeneous *Eucalyptus urograndis* plantations and observed only marginal differences in the predictive performances of NN and PPM. The advantage of the PPM approach is that it can be applied with a smaller training dataset whereas NN always requires a comprehensive training data.

The NN approach may be used to create a wall-to-wall map of the DBH distribution. Such maps for other forest attributes, based on NFI and remotely sensed data are publicly available, for example, in Sweden (Nilsson et al. 2017) and Finland (Kangas et al. 2017), and Norway (Astrup et al. 2019). In MA estimation, systematic errors in the predicted forest attribute maps are mitigated. This is a crucial step as can be seen from the non-zero correction factors utilized in the MA estimator.

To the best of our knowledge, the efficiency of the MA estimation of DBH distributions or total stem frequencies using a combination of field and remotely sensed data has not been reported so far (Magnussen and Renaud 2016). Our findings showed that the estimates for the DBH classes on the left tail of distribution profited considerably from using remotely-sensed data. However, also RE values even slightly greater than 1.00 mean a considerable improvement in large-scale inventories with thousands of field plots. For example, an RE value of 1.30 associated with the model-assisted estimator in our case means that approximately 2,880 additional field plots and thus a significant investment would be required to achieve the same precision. Here, we estimated DBH distributions with a bin width of 2 cm which is a detailed characterization from the point of view of strategic forest inventories. Bigger DBH classes resulted in larger RE values (results not shown) which also fits to the considerable larger RE value associated with the total stem frequency compared with RE values of 2 cm DBH classes.

The efficiency gain achieved by the MA estimation may also increase if the accuracy of the forest mask and tree species map could be improved in the future.

6 CONCLUSIONS

The following conclusions can be drawn from this study: i) The GLM approach outperformed the PPM approach, although the differences in the errors of predicted DBH distributions were small; ii) the NN approach clearly outperformed the parametric GLM and PPM approaches; iii) The utilization of NN predictions in the model-assisted estimation of the DBH distribution resulted in considerable efficiency gains.

ACKNOWLEDGEMENTS

We would like to thank Marius Hauglin, Johannes Rahlf, and Johannes Schumacher for their support in data preparation and processing.

APPENDIX

Table A1. Parameter estimates and their standard errors/confidence intervals (SE/CI) associated with the linear mixed-effects models (PPM) for Weibull scale and shape parameters. Please refer to Table 2 for the abbreviations of predictor variables. L – lower bound, U – upper bound

Pine-dominated				Deciduous-dominated					
scale		shape		scale		shape			
Est.	SE	Est.	SE	Est.	SE	Est.	SE		
Intercept	3.53	1.05	1.33	0.17	Intercept	5.74	0.91	1.94	0.16
d4 _{all}	6.12	2.52	-	-	igratio _{all}	1.21	1.21	-	-
h90 _{all}	0.96	0.08	-	-	h50 _{all}	0.24	0.24	-	-
h50 _{last}	-0.60	0.13	-	-	hvar _{first}	0.20	0.20	0.26	0.01
hmean _{all}	-	-	-0.30	0.05	d8 _{first}	-	-	3.69	1.10
hvar _{all}	-	-	0.06	0.01	h75 _{first}	-	-	-0.09	0.026
d6 _{first}	-	-	3.34	0.77	-	-	-	-	-
Est.		95% CI		Est.		95% CI			
		[L, U]		[L, U]		[L, U]			
σ_b *	1.86	[1.27, 2.74]	0.36	[0.21, 0.60]	σ_b *	1.46	[0.70, 3.06]	0.17	[0.02, 1.53]
σ	6.08	[5.76, 6.41]	1.43	[1.36, 1.51]	σ	4.55	[4.08, 5.06]	0.98	[0.88, 1.09]

* Note: ALS project-area random effect

Table A2. Parameter estimates and their standard errors/confidence intervals (SE/CI) associated with the generalized linear models (GLM) for Weibull scale and shape parameters. Please refer to Table 2 for the abbreviations of predictor variables. L – lower bound, U – upper bound

Pine-dominated				Deciduous-dominated					
scale		shape		scale		shape			
Est.	SE	Est.	SE	Est.	SE	Est.	SE		
Intercept	2.17	0.02	0.32	0.17	Intercept	1.91	0.02	0.51	0.02
d4 _{all}	0.12	0.04	-	-	igratio _{all}	0.05	0.01	-	-
h90 _{all}	0.05	<0.01	-	-	h50 _{all}	0.02	<0.01	-	-
h50 _{last}	-0.03	<0.01	-	-	hvar _{first}	0.02	<0.01	<0.01	<0.01
hmean _{all}	-	-	-0.06	<0.01	d8 _{first}	-	-	1.46	0.12
hvar _{all}	-	-	0.01	<0.01	h75 _{first}	-	-	-0.02	<0.01
d6 _{first}	-	-	1.26	0.08	-	-	-	-	-
Est.		95% CI		Est.		95% CI			
		[L, U]		[L, U]		[L, U]			
σ_b *	0.22	[0.21, 0.23]	0.31	[0.30, 0.33]	σ_b *	0.23	[0.21, 0.26]	-	-

* Note: plot-level random effect for GLM, random effect was not used for the shape model in

the deciduous-dominated plots.

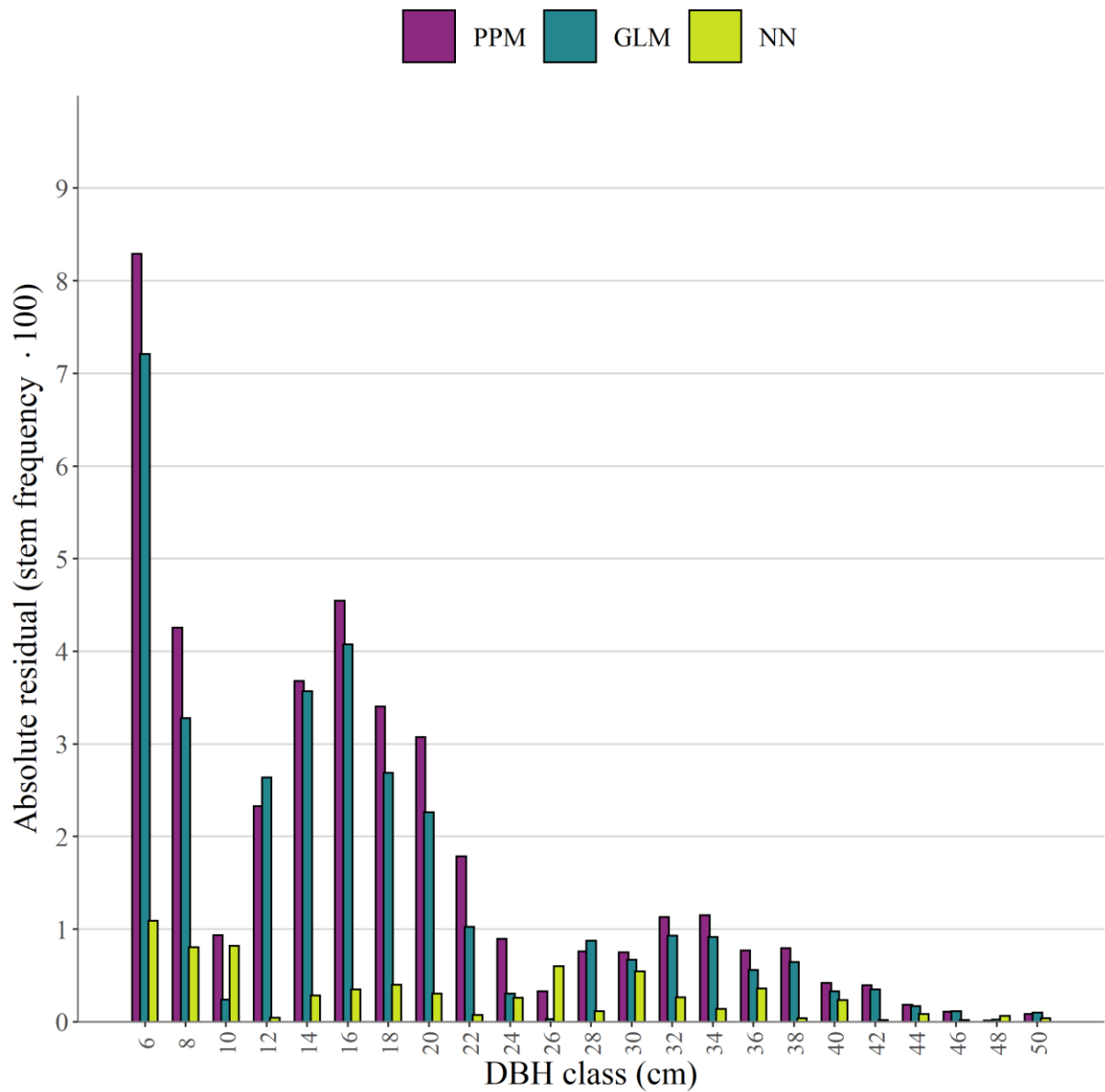


Figure A1. Absolute residuals of DBH distribution summed over all pine-dominated plots (n = 813, modeling dataset). PPM – parametric prediction method with linear mixed-effects models, GLM – generalized linear model

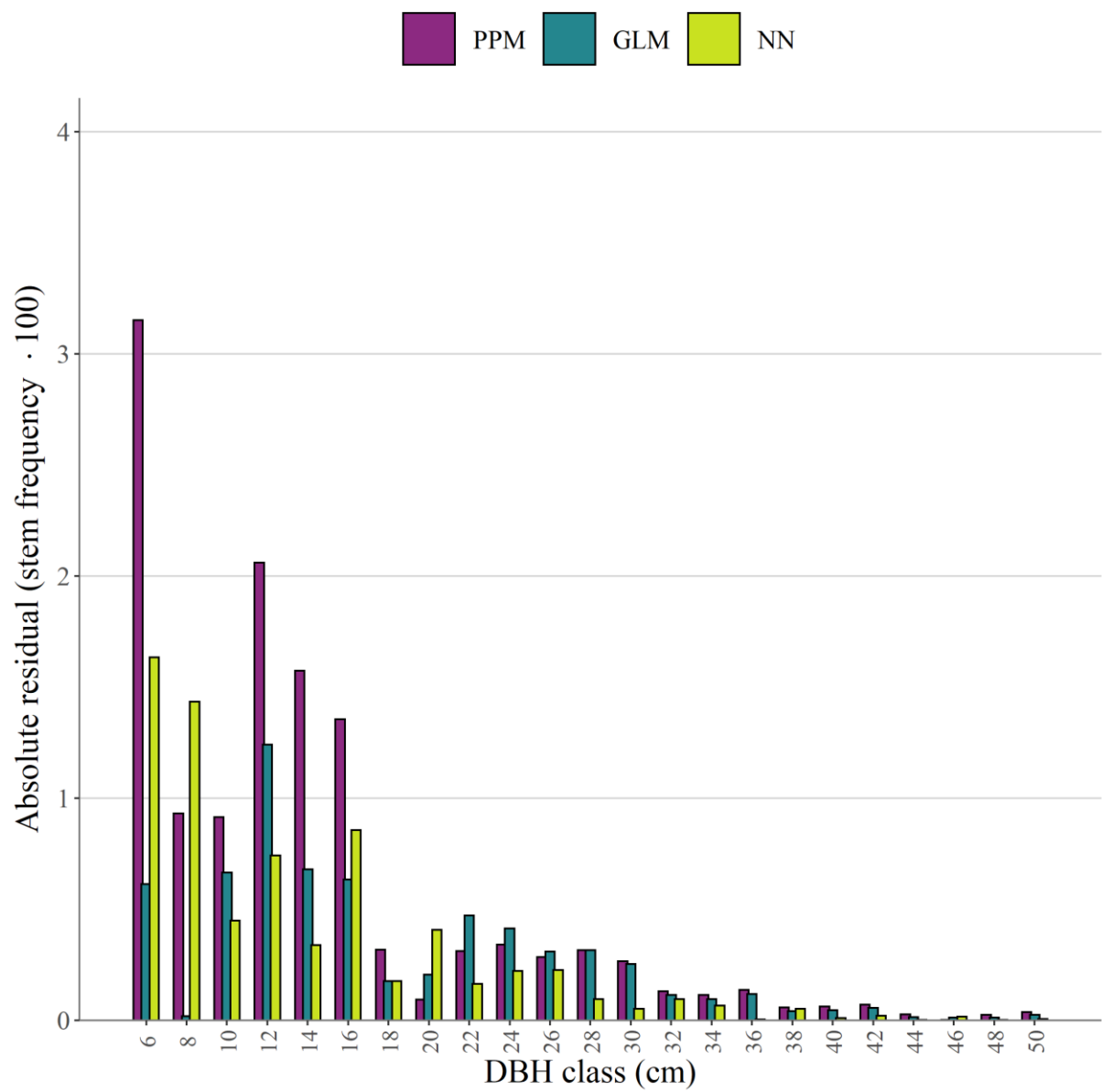


Figure A2. Absolute residuals of DBH distribution summed over all deciduous-dominated plots (n = 259, modeling dataset). PPM – parametric prediction method with linear mixed-effects models, GLM – generalized linear model

REFERENCES

Astrup, R., Rahlf, J., Bjørkelo, K., Debella-Gilo, M., Gjertsen, A.-K., and Breidenbach, J. 2019. Forest information at multiple scales: development, evaluation and application of the Norwegian forest resources map SR16. *Scand. J. For. Res.* 34(6): 484–496. doi:10.1080/02827581.2019.1588989.

Bailey, R.L., and Dell, T.R. 1973. Quantifying diameter distributions with the Weibull function. *For. Sci.* 19(2): 97–104. doi:10.1093/forestscience/19.2.97.

Breidenbach, J., Gläser, C., and Schmidt, M. 2008. Estimation of diameter distributions by means of airborne laser scanner data. *Can. J. For. Res.* 38(6): 1611–1620. doi://dx.doi.org/10.1139/x07-237.

Breidenbach, J., Næsset, E., and Gobakken, T. 2012. Improving k-nearest neighbor predictions in forest inventories by combining high and low density airborne laser scanning data. *Remote Sens. Environ.* 117: 358–365. doi:10.1016/j.rse.2011.10.010.

Breidenbach, J., Granhus, A., Hylen, G., Eriksen, R., and Astrup, R. 2020a. A century of National Forest Inventory in Norway – informing past, present, and future decisions. *For. Ecosyst.* 7(1): 46. doi:10.1186/s40663-020-00261-0.

Breidenbach, J., Waser, L.T., Debella-Gilo, M., Schumacher, J., Rahlf, J., Hauglin, M., Puliti, S., and Astrup, R. 2020b. National mapping and estimation of forest area by dominant tree species using Sentinel-2 data. *Can. J. For. Res.* doi:10.1139/cjfr-2020-0170.

Burk, T.E., and Newberry, J.D. 1984. A simple algorithm for moment-based recovery of Weibull distribution parameters. *For. Sci.* 30(2): 329–332. doi:10.1093/forestscience/30.2.329.

Cao, Q.V. 2004. Predicting parameters of a Weibull function for modeling diameter distribution. *For. Sci.* 50(5): 682–685. Oxford Academic. doi:10.1093/forestscience/50.5.682.

Coomes, D.A., and Allen, R.B. 2007. Mortality and tree-size distributions in natural mixed-age forests. *J. Ecol.* 95(1): 27–40. doi:10.1111/j.1365-2745.2006.01179.x.

Crookston, N.L., and Finley, A.O. 2008. yaImpute: An R Package for kNN Imputation. *J. Stat. Softw.* 23(1): 1–16. doi:10.18637/jss.v023.i10.

Fahrmeier, L., Kneib, T., Lang, S., and Marx, B. 2013. Regression models, methods and applications. In 1st edition. Springer-Verlag, Berlin Heidelberg.

Gobakken, T., and Næsset, E. 2004. Estimation of diameter and basal area distributions in coniferous forest by means of airborne laser scanner data. *Scand. J. For. Res.* 19(6): 529–542. doi:10.1080/02827580410019454.

Hafley, W.L., and Schreuder, H.T. 1977. Statistical distributions for fitting diameter and height data in even-aged stands. *Can. J. For. Res.* 7(3): 481–487. doi:10.1139/x77-062.

Haakana, H., Heikkinen, J., Katila, M., and Kangas, A. 2020. Precision of exogenous post-stratification in small-area estimation based on a continuous national forest inventory. *Can. J. For. Res.* 50(4): 359–370. doi:10.1139/cjfr-2019-0139.

Henttonen, H.M., Nöjd, P., Suvanto, S., Heikkinen, J., and Mäkinen, H. 2020. Size-class structure of the forests of Finland during 1921–2013: a recovery from centuries of exploitation, guided by forest policies. *Eur. J. For. Res.* 139(2): 279–293. doi:10.1007/s10342-019-01241-y.

Hynynen, J., Ojansuu, R., Hökkä, H., Siipilehto, J., Salminen, H., and Haapala, P. 2002. Models for predicting stand development in MELA System. Metsätutkimuslaitos. Available from <http://jukuri.luke.fi/handle/10024/521469> [accessed 22 January 2019].

Kangas, A., Astrup, R., Breidenbach, J., Fridman, J., Gobakken, T., Korhonen, K.T., Maltamo, M., Nilsson, M., Nord-Larsen, T., Næsset, E., and Olsson, H. 2018. Remote sensing and forest

inventories in Nordic countries – roadmap for the future. *Scand. J. For. Res.* 33(4): 397–412. doi:10.1080/02827581.2017.1416666.

Kartverket. 2019. Høydedata og terrengmodeller for landområdene. Available from <https://www.kartverket.no/data/Hoydedata-og-terrengmodeller/> [accessed 11 March 2020].

Kilkki, P., Maltamo, M., Mykkänen, R., and Päivinen, R. 1989. Use of the Weibull function in estimating the basal area dbh-distribution. *Silva Fenn.* 23(4). doi:10.14214/sf.a15550.

Kirkpatrick, S., Gelatt, C.D., and Vecchi, M.P. 1983. Optimization by simulated annealing. *Science* 220(4598): 671–680. doi:10.1126/science.220.4598.671.

Loetsch, F., Zöhrer, F., and Haller, K.E. 1973. Forest inventory 2. : 469.

Magnussen, S., and Renaud, J.-P. 2016. Multidimensional scaling of first-return airborne laser echoes for prediction and model-assisted estimation of a distribution of tree stem diameters. *Ann. For. Sci.* 73(4): 1089–1098. doi:10.1007/s13595-016-0581-2.

Maltamo, M., Næsset, E., Bollandsås, O.M., Gobakken, T., and Packalén, P. 2009. Non-parametric prediction of diameter distributions using airborne laser scanner data. *Scand. J. For. Res.* 24(6): 541–553. doi:10.1080/02827580903362497.

Maltamo, M., and Packalen, P. 2014. Species-Specific Management Inventory in Finland. In *Forestry Applications of Airborne Laser Scanning: Concepts and Case Studies*. Edited by M. Maltamo, E. Næsset, and J. Vauhkonen. Springer Netherlands, Dordrecht. pp. 241–252. doi:10.1007/978-94-017-8663-8_12.

Maltamo, M., Mehtätalo, L., Valbuena, R., Vauhkonen, J., and Packalen, P. 2018. Airborne laser scanning for tree diameter distribution modelling: a comparison of different modelling alternatives in a tropical single-species plantation. *Forestry* 91(1): 121–131. doi:10.1093/forestry/cpx041.

Mauro, F., Frank, B., Monleon, V.J., Temesgen, H., and Ford, K. 2019. Prediction of diameter distributions and tree-lists in southwestern Oregon using LiDAR and stand-level auxiliary information. *Can. J. For. Res.* doi:10.1139/cjfr-2018-0332.

McRoberts, R., and Tomppo, E. 2007. Remote sensing support for national forest inventories. *Remote Sens. Environ.* 110(4): 412–419. doi:10.1016/j.rse.2006.09.034.

McRoberts, R.E., Næsset, E., and Gobakken, T. 2013. Inference for lidar-assisted estimation of forest growing stock volume. *Remote Sens. Environ.* 128: 268–275. doi:10.1016/j.rse.2012.10.007.

Mehtätalo, L., Maltamo, M., and Packalén, P. 2007. Recovering plot-specific diameter distribution and height-diameter curve using ALS based stand characteristics. ISPRS Workshop on Laser Scanning 2007 and SilviLaser 2007, September 12-14, Espoo, Finland.

Mehtätalo, L., and Lappi, J. 2020. Biometry for forestry and environmental data with examples in R. CRC press.

Moeur, M., and Stage, A.R. 1995. Most similar neighbor: An improved sampling inference procedure for natural resource planning. *For. Sci.* 41(2): 337–359. doi:10.1093/forestscience/41.2.337.

Nilsson, M., Nordkvist, K., Jonzén, J., Lindgren, N., Axensten, P., Wallerman, J., Egberth, M., Larsson, S., Nilsson, L., Eriksson, J., and Olsson, H. 2017. A nationwide forest attribute map of Sweden predicted using airborne laser scanning data and field data from the National Forest Inventory. *Remote Sens. Environ.* 194: 447–454. doi:10.1016/j.rse.2016.10.022.

Næsset, E. 1997. Estimating timber volume of forest stands using airborne laser scanner data. *Remote Sens. Environ.* 61(2): 246–253. doi:10.1016/S0034-4257(97)00041-2.

Næsset, E. 2014. Area-based inventory in Norway – From innovation to an operational reality. In *Forestry applications of airborne laser scanning: Concepts and case studies*. Edited by M. Maltamo, E. Næsset, and J. Vauhkonen. Springer Netherlands, Dordrecht. pp. 215–240. doi:10.1007/978-94-017-8663-8_11.

Packalén, P., and Maltamo, M. 2008. Estimation of species-specific diameter distributions using airborne laser scanning and aerial photographs. *Can. J. For. Res.* 38(7): 1750–1760. doi:10.1139/X08-037.

Packalén, P., Temesgen, H., and Maltamo, M. 2012. Variable selection strategies for nearest neighbor imputation methods used in remote sensing based forest inventory. *Can. J. Remote Sens.* 38(5): 557–569. doi:10.5589/m12-046.

R Core Team. 2020. R: A language and environment for statistical computing. R Foundation for Statistical Computing. Available from <https://www.R-project.org/>.

Rigby, R.A., and Stasinopoulos, D.M. 2005. Generalized additive models for location, scale and shape. *Journal of the Royal Statistical Society: Series C (Applied Statistics)* 54(3): 507–554. doi:10.1111/j.1467-9876.2005.00510.x.

Rouvinen, S., and Kuuluvainen, T. 2005. Tree diameter distributions in natural and managed old *Pinus sylvestris*-dominated forests. *For. Ecol. Manag.* 208(1): 45–61. doi:10.1016/j.foreco.2004.11.021.

Siipilehto, J., and Mehtätalo, L. 2013. Parameter recovery vs. parameter prediction for the Weibull distribution validated for Scots pine stands in Finland. *Silva Fenn.* 47(4). doi:10.14214/sf.1057.

Strunk, J.L., Gould, P.J., Packalen, P., Poudel, K.P., Andersen, H.-E., and Temesgen, H. 2017. An examination of diameter density prediction with k-NN and airborne lidar. *Forests* 8(11): 444. *Forests*. doi:10.3390/f8110444.

Thomas, V., Oliver, R.D., Lim, K., and Woods, M. 2008. LiDAR and Weibull modeling of diameter and basal area. *For. Chron.* 84(6): 866–875. doi:10.5558/tfc84866-6.

Valbuena, R., Packalen, P., Mehtätalo, L., García-Abril, A., and Maltamo, M. 2013. Characterizing forest structural types and shelterwood dynamics from Lorenz-based indicators predicted by airborne laser scanning. *Can. J. For. Res.* 43(11): 1063–1074. doi:10.1139/cjfr-2013-0147.

Zhang, L., Gove, J.H., Lie, C., and Leak, W.B. 2001. A finite, mixture of two Weibull distributions for modeling the diameter distributions of rotated-sigmoid, uneven-aged stands. *Can. J. For. Res.* 31(9): 1654–1659.

Zutter, B.R., Oderwald, R.G., Murphy, P.A., and Farrar, R.M. 1986. Characterizing diameter distributions with modified data types and forms of the Weibull distribution. *For. Sci.* 32(1): 37–48.